Determination of Filter-Cake Thicknesses from On-Line Flow Measurements and Gas/Particle Transport Modeling

Duane H. Smith, (DSMITH@metc.doe.gov; 304-285-4069), U. S. Department of Energy, Morgantown Energy Technology Center, Morgantown, WV 26507-0880,

Victor Powell, (powell@stat.duke.edu) ORISE Faculty participant at U. S. Department of Energy, Morgantown Energy Technology Center, Morgantown, WV 26507-0880,

Martin Ferer, (FERER@wvums.wvnet.edu, 304-293-3422), Department of Physics, West Virginia University, Morgantown, WV 26506,

Goodarz Ahmadi, (AHMADI@sun.soe.clarkson.edu, 315-268-2322), National Research Council Senior Associate at U. S. Department of Energy, Morgantown Energy Technology Center, Morgantown, WV 26507-0880, and

Essam Ibrahim (emeei@acd.tusk.edu, 334-727-8974), ORISE Faculty participant at U. S. Department of Energy, Morgantown Energy Technology Center, Morgantown, WV 26507-0880

INTRODUCTION

The use of cylindrical candle filters to remove fine (~0.005 mm) particles from hot (~500-900 ^{o}C) gas streams currently is being developed for applications in advanced pressurized fluidized bed combustion (PFBC) and integrated gasification combined cycle (IGCC) technologies. Successfully deployed with hot-gas filtration, PFBC and IGCC technologies will allow the conversion of coal to electrical energy by direct passage of the filtered gases into non-ruggedized turbines and thus provide substantially greater conversion efficiencies with reduced environmental impacts [1].

In the usual approach, one or more clusters of candle filters are suspended from a tubesheet in a pressurized (P ~< 1 MPa) vessel into which hot gases and suspended particles enter, the gases pass through the walls of the cylindrical filters, and the filtered particles form a cake on the outside of each filter ([2-4]). The cake is then removed periodically (typically, two or three times per hour), by a backpulse of compressed air from inside the filter, which passes through the filter wall and filter cake.

In various development or demonstration systems the thickness of the filter cake has proved to be an important, but unknown, process parameter. For example, the distance between adjacent filters typically is on the order of 5 cm. If the filter-cake thickness should reach 2.5 cm, "bridging" of cake between adjacent filters would occur, leaving little space between the filters into which the incoming gases and particles could flow. Bridging might eventually occur if the removal of cake at each cleaning were not quite complete, or if a fraction of the particles removed were re-entrained and refiltered after each cleaning backpulse.

The accumulation of particulates around and among filters is not just a hypothetical concern. Operating experience with the Tidd PFBC Demonstration Plant revealed that under some conditions the buildup of large masses of particulates among the filters can, indeed, be an important problem, producing excessive pressure drops within the filter vessel and even filter breakage [5].

Because of the high temperatures and pressures, the geometries of the filter clusters and mechanical supports, and the presence of fine particles to scatter any light, on-line measurement of cake thicknesses during filter-system operation has not been feasible in most systems. However, when the pressure drop across the filter tubesheet, the gas flow rate, and the particle concentration in the incoming gases are measured, these data can be used to calculate the mass of filter cake on each filter. If filter-cake samples can be obtained (e.g., from the filter-vessel hopper or during shut-down) so that the filter cake porosity can be measured, then the filter-cake thickness can be estimated during plant operation, as well. In a typical filter system, the needed flow data are logged and the cake thickness can be estimated several times per minute, so that the filter system need not be operated "blindly," without knowledge of the extent of cake buildup.

The following section describes a physical model for cake and pressure buildups between cleaning backpulses, and for longer term buildups of the "baseline" pressure drop, as caused by incomplete filter cleaning and/or re-entrainment. When combined with operating data and laboratory measurements of the cake porosity, the model may be used to calculate the (average) filter permeability, the filter-cake thickness and permeability, and the fraction of filter-cake left on the filter by the cleaning backpulse or re-entrained after the backpulse.

When used for a variety of operating conditions (e.g., different coals, sorbents, temperatures, etc.), the model eventually may provide useful information on how the filter-cake properties depend on the various operating parameters.

MODELS

Consider a filter vessel with *n* candle filters. For each filter, the gas flows through the filter cake, then through the filter wall, so that the *i*th filter and the corresponding filter cake constitute two resistances in series:

$$ {}^{i}R_p = {}^{i}R_f + {}^{i}R_c. \qquad (1) $$

All *n* filters (and their cakes) operate in parallel and are subjected to the same pressure drop. Thus their effective resistance R is given as:

$$ 1/R = \Sigma(1/{}^{i}R_p). \qquad (2) $$

The net, measured pressure drop is the sum of the pressure drop across filters and filter cakes and the pressure drop through other flow paths in the filtration system. Therefore, the net vessel resistance R_n is:

$$ R_n = R + R_o, \qquad (3) $$

where R_o is the passage resistance. It should be noted here that the passage resistance is, in general, a function of flow rate.

The model used here makes the following assumptions: (1) all *n* filters have the same permeability; (2) essentially all particles that enter the filter vessel are deposited on the filters; (3) the particles are distributed uniformly among the filters and on each filter surface; and (4) the filter cakes (as well as the filters) obey Darcy's law,

$$\mathbf{v} = (k/\mu)\nabla P, \tag{4}$$

where **v** is the velocity vector, P is the pressure and k is the permeability.

To simplify the model, the small area at the bottom of the filter (about 1% of the total filter surface), for which the gas flow rate differs significantly from the rest of the filter, is ignored in the subsequent analysis. Under assumptions (1)-(3), ${}^{i}R_f$ and ${}^{i}R_c$ are the same for all *n* filters, and eq (3) reduces to

$$R_n = (1/n)(R_f + R_c) + R_o. \tag{5}$$

Because of the cylindrical geometry of the filters and filter cakes, Darcy's law is solved in polar coordinates. Assuming that the pressure varies only radially, the resulting pressure drop across each clean candle filter (in the absence of filter cake) is (Yang et al.[4]):

$$\Delta P_f = (1/2\pi k_f)\mu (Q/nh)\ln(b/a), \tag{6}$$

where Q is the vessel (volumetric) gas flow rate, k_f is the filter permeability, *h* is the filter length, and *a* and *b* are the inside and outside radii of the filter wall, respectively.

At constant gas flow rate into the filter vessel, *Q*, and constant volume fraction of particles in the incoming gas, *F*, the volume of filtered particles per filter that arrives in the filter vessel during time interval *t* is

$$V = FQt/n. \tag{7}$$

The corresponding volume of each filter cake is

$$V(t) = FQt/n(1- \phi) \tag{8}$$

where ϕ is porosity of the cake. The outer radius of the filter cake , B(t), at time t then is given by

$$B(t) = b[1 + FQt/\pi nh(1- \phi)b^2]^{1/2}. \tag{9}$$

The increase in the pressure drop across the filter cakes over the time interval from $t = 0$ to time t is

$$\Delta P_c(t) = (1/4\pi k_c)\mu(Q/nh) \ln [1 + FQt/nh\pi(1- \phi)b^2], \quad (10)$$

where k_c is the filter-cake permeability. Typically the filters are cleaned periodically after interval t' ($t' \sim 20$ to 60 min) with a backpulse of compressed air of about 0.2 s duration. In eq (10), t is the time measured after the backpulse.

Ideal operation

In the simplest case, cleaning of the filters by the backpulse is complete and no "re-entrainment" (i.e., refiltration) of any of the cake occurs. At time $t = 0$ the filter cake thickness is zero, and the pressure drop $\Delta P - \Delta P_o$ arises only from the clean filters:

$$\Delta P - \Delta P_o = (1/2\pi k_f)\mu(Q/nh) \ln(b/a). \quad (11)$$

Over the time interval $t = 0$ to $t = t'$ filtration occurs, and

$$\Delta P - \Delta P_o = \mu(Q/2\pi nh)\{(1/k_f) \ln(b/a) + (1/2k_c) \ln [1 + FQt/nh\pi(1- \phi)b^2]\}. \quad (12)$$

At $t = t'$ the backpulse occurs, and $\Delta P - \Delta P_o$ becomes negative. Because cake removal is complete and no re-entrainment occurs, after the backpulse the pressure drop returns to the initial value for the clean filters:

$$\Delta P(t = t') - \Delta P_o = \Delta P(t = 0) - \Delta P_{o,} \quad (13)$$

[where $\Delta P(t = 0) - \Delta P_o$ is given by eq (11)]. During the second cycle and all subsequent cycles, the cake buildup, pressure buildup, and cleaning of the first cycle are simply repeated.

If the flow that produces ΔP_o in various passages is turbulent and

$$\Delta P_o = cQ^2, \quad (14)$$

the value of c can be obtained from pressure drops measured at different flow rates. Then, from on-line measurements of F and Q (and of the temperature, to get μ), and from laboratory measurements of the filter dimensions (a, b, h) and cake porosity (ϕ), fits of eq (12) to the experimental data yield the filter permeability (k_f), the filter-cake permeability (k_c), and the thickness of the filter cake

$$\delta = B(t) - b = b\{[1 + Fqt/\pi nh(1-\phi)b^2]^{1/2} - 1\} \quad (15)$$

at any time.

Incomplete cleaning

If the performance of filter systems always conformed to the ideal case, there would be little need to determine filter-cake permeabilities and thicknesses during system operation. However, all too often, filter systems do not exhibit ideal behavior. It seems unavoidable that, after each cleaning, some portion of the cake will remain on the filter and/or some of the fragments of filter cake removed by the backpulse will be recollected on the filter surface. Intuitively, it also may appear inevitable that the thickness of the "residual" cake from incomplete cleaning and re-entrainment must increase without limit, until all of space between adjacent filters is filled and bridging occurs.

Imagine that an outer cylinder of cake of uniform thickness is removed by the *j*th backpulse, leaving a uniform cake of outer radius B_j on the filter at the beginning of the *j*th + 1 cycle. Hence, at the start of the *j*th + 1 cycle the pressure drop is no longer $\Delta P - \Delta P_o = \Delta P_f = (1/2\pi k_f)\mu(Q/nh)\ln(b/a)$ [eq (11)], but

$$\Delta P - \Delta P_o = (1/2\pi)\mu(Q/nh)\,[\ln(b/a)/k_f + \ln(B_j/b)/k_c]. \qquad (16)$$

If the incremental thickness of cake left on the filter after each cleaning is a constant fraction, $^r f$, of the cake deposited *during that cycle*, then

$$\Delta B_j = \Delta B = {}^r f\,(B' - b), \qquad (17)$$

where $B' = B(t=t')$ is the radius of the cake at the end of the first cycle. Assuming that the deposited cake thickness for different cycle is essentially constant, at the beginning of the *j*th+1 cycle the cake thickness is

$$B - b = j\,{}^r f\,(B' - b), \qquad (18)$$

and

$$\Delta P - \Delta P_o = (1/2\pi)\mu(Q/nh)\{(1/k_f)\ln(b/a) + (1/k_c)\ln[j\,{}^r f\,(B' - b)/b + 1]\}. \qquad (19)$$

After $j = 1/{}^r f$ cycles the thickness of the residual cake left after the filter cleaning is equal to the thickness of the cake deposited just before the first cleaning backpulse. Thus, unless $^r f$ is very small, the cake thickness quickly becomes many times as large as the thickest cake ever encountered in the ideal case. In normal operation $B_{max} - b >> B' - b$, where B_{max} is the maximum possible filter-cake thickness (less than half the nearest neighbor distance between filters). Hence, if $^r f$ = constant, satisfactory operation requires

$$T_s < (t'/{}^r f)\,(B_{max} - b)/(B' - b) \qquad (20)$$

where T_s is the time of operation before the filter vessel must be opened and manually cleaned.

Re-entrainment.

In refiltration, or re-entrainment, the removal of filter cake by the cleaning backpulse is complete, but some fraction of the resulting filter-cake fragments return to the filter surface. The fraction of re-entrained particles is a function of the size distribution of the cake fragments: fragments that are sufficiently large move downward under the force of gravity and tend to escape; fragments that are not much larger than the largest particles entering the vessel have a high probability of being re-entrained. The new locations of these fragments on the filters may be different from their location before the backpulse, but these fragments will be refiltered within a short time after the backpulse occurs.

The mass (or volume) of particles and filter cake re-filtered during the *j*th filtration cycle will be some fraction, f_j, of the total mass of cake removed by the *j*th - 1 backpulse. By the end of the first cycle a mass of cake ${}^{e}m_1 = m' = \rho FQt/n$ (and volume ${}^{e}V_1 = V' = FQt'/n(1-\phi)$ [eq (8)]) forms on each filter, which causes a pressure increase

$$ {}^{e}(\Delta P)_1 = \Delta P' = \Delta P(t'), \tag{21} $$

as given by eq (10). Within a short while after the first cleaning backpulse an amount

$$ {}^{i}m_2 = f_2 m' \tag{22a} $$

of blown-off cake fragments is recaptured on each filter, which causes an increased pressure drop

$$ {}^{i}(\Delta P)_2 = f_2\ \Delta P'. \tag{22b} $$

Here f_2 is the fraction recaptured; and it is assumed that, for small f's, the increase in pressure drop is proportional to the increase in cake radius. During the second cycle an amount m' of freshly filtered particles is added to the cake already present from re-entrainment, so that at the end of the second cycle (just before the cleaning backpulse) the mass of filter cake is

$$ {}^{e}m_2 = m' + f_2 m' = (1 + f_2)\ m' \tag{22c} $$

and the pressure drop is

$$ {}^{e}(\Delta P)_2 = (1 + f_2)\ \Delta P' \tag{22d} $$

After the second backpulse and the re-entrainment at the beginning of cycle 3, the cake-mass is

$$ {}^{i}m_3 = f_3(1 + f_2)\ m' \tag{23a} $$

and the pressure drop is

$$^{i}(\Delta P)_3 = f_3(1 + f_2)\ \Delta P'. \tag{23b}$$

At the end of cycle 3 the filter-cake mass and the pressure drop are, respectively,

$$^{e}m_{\ 3} = [1 + f_{\ 3}(1 + f_2)]m' \tag{23c}$$

and

$$^{e}(\Delta P)_3 = [1 + f_{\ 3}(1 + f_2)]\Delta P'. \tag{23d}$$

For the *j*th cycle the recaptured cake-mass is

$$^{i}m_j = (f_j + f_j f_{j\ -1} + f_j f_{j\ -1} f_{j\ -2} + \ldots + f_j f_{j\ -1}\ \ldots f_3 f_2)m' \tag{24a}$$

and the increase in pressure drop is

$$^{i}(\Delta P)_j = (f_j + f_j f_{j\ -1} + f_j f_{j\ -1} f_{j\ -2} + \ldots + f_j f_{j\ -1} \ldots f_3 f_2)\Delta P' \tag{24b}$$

At the end of the *j*th cycle the filter-cake mass and the pressure drop are, respectively,

$$^{e}m_j = (1 + f_j + f_j f_{j\ -1} + f_j f_{j\ -1} f_{j\ -2} + \ldots + f_j f_{j\ -1} \ldots f_3 f_2)m' \tag{24c}$$

and

$$^{e}(\Delta P)_j = (1 + f_j + f_j f_{j\ -1} + f_j f_{j\ -1} f_{j\ -2} + \ldots + f_j f_{j\ -1} \ldots f_3 f_2)\Delta P'. \tag{24d}$$

These quantities define the "baseline" and "topline" of the pressure drop versus time. Thus, eqs (22b) and (22d) may be used with the pressure drops measured at the beginning and end, respectively, of the second cycle to give "duplicate" measurements of f_2; the "best" value of f_2, along with eqs (23b) and (23d) and the pressure drops measured at the beginning and end of the third cycle give "duplicate" measurements of f_3; etc.

A plausible hypothesis is that the fraction of filter cake re-entrained during each cycle should be constant for all cycles. With this hypothesis eq (24d) reduces to

$$^{e}(\Delta P)_j = (1 + f + f^{\,2} + \ldots + f^{\,j-1})\Delta P' \tag{25}$$

As the number of cycles becomes very large ($j \Rightarrow$ infinity), the maximum pressure drop encountered at the beginning of each cycle is

$$^{e}(\Delta P) = \Delta P'/(1-f), \tag{26}$$

where $0 \leq f < 1$ is assumed.

RESULTS

Figure 1 shows the variation of the ratio of pressure drop to flow rate versus time for fifteen one-hour cycles of operation of the "MGCR" filter vessel. The corresponding time variation of the flow rate through the vessel is shown in Figure 2. (The units are pressure drop [ΔP] = lb/in^2, flow rate [Q] = scfh, and time [t] = s.) The roughly linear buildup of pressure drop after each backpulse is clearly observed from Figure 1. The flow rate appears to be steady with some random variations. At about 15,000 s, there is a step change of about 10 percent in the mean flow rate. For t < 15,000 s, a portion of the gas from the gasification unit was sampled for particle concentration measurements, while for larger times, the entire flow was passed through the filter vessel. During the transition, some adjustment of the operation was also required. As a result, the pressure variation in the fifth cycle shows an abnormal behavior.

Ideal operation

If only a few filtration/cleaning cycles are monitored, the operation of the filter system may appear ideal upon casual inspection. To clearly illustrate the details of the pressure drop buildup and its sharp reduction during the backpulse, a set of operational data, $\Delta P/Q$ versus t, for three cycles of the filter vessel of the MGCR (gasification) unit are shown in in Figure 3. The apparent constancy of the baseline values seems to indicate that no incomplete cleaning or re-entrainment occurred (unless an asymptotic limit for re-entrainment had been nearly reached).

Laboratory measurements showed that the filter cake had high porosity. Here a porosity of $\phi = 0.6$ for the filter cake is assumed, and a least-square error fit of the ideal operation model [eq (12)] to the data for the fifteen cycles (of 54,000 s duration) is evaluated. The resulting expression is given as

$$\Delta P_j/Q = 0.00135 + 0.003097 \ln [1 + 3.67 \times 10^{-8} Qt], \qquad (27)$$

where the operation condition units are used.

The predictions of equation (27) for the three and the fifteen cycles are plotted in Figures 4 and 5, respectively. Comparing Figures 1 and 3 with 4 and 5, it is readily apparent that the ideal operation model provides a reasonable fit to the data. By including the time variations of the flow rate, it was even possible to predict some of the "noise" in the operating pressure drop data. Here the statistical R^2-value is 0.78 (which indicates that roughly 78 percent of the data are explained by the ideal model).

A more detailed check on the statistical fit of the model is provided by Figure 6. This figure illustrates the statistical residual [measured value minus value calculated from the fit] for each of the individual measured values. The observed low level of residual indicates that the statistical fit is quite good. The very largest residuals correspond to the sporadic fluctuations in the detectors and/or other system "noise." It also appears from Figure 6 that the residuals for the first 15,000 s with lower flow rate are positive, while those for the larger times are negative. There is also a high level of residual for the fifth cycle, which is as expected from the operational changes made at that time.

The coefficient of the logarithm term in eq (12) is related to the cake permeability. The correlation given by eq (27) may then be used to estimate k_c. Accordingly, the estimated cake permeability is 8.8×10^{-13} m^2, which is in the expected range. The cake thickness may also be evaluated from equation (9) as a function of time, under the idealized cleaning assumption. For a gas flow rate of 2,000 scfh, the corresponding peak cake thickness at the end of an ideal cycle (with complete cleaning after each backpulse) becomes $B(t') - b \approx 4$ mm.

In spite of the reasonable agreement, one feature of the ideal model prediction is noticeably different from the experimental data. Figures 4 and 5 show that the model leads to an identical pressure drop level after each backpulse, while Figure 1 indicates a random deviation in the baseline pressure drop due to incomplete cleaning, re-entrainment and/or removal of some additional residual filter cake deposited in the earlier cycles. The ideal model was extended to account for the effect of initial variation of the pressure drop after each backpulse. The resulting best statistical fit to the data then is given as

$$\Delta P_j/Q = 0.001526 + 0.003172 \ln [1 + 3.67 \times 10^{-8} Qt] - \Theta_j, \qquad (28)$$

where $\Theta_j = [^i(\Delta P_j) - {}^i(\Delta P_{j-1})]/Q$ is the change in the base pressure drop (divided by the flow rate) just after the backpulse for the *jth* cycle. With an average of $\Theta_{ave} = - 1.06 \times 10^{-5}$, the values of Θ vary from -1.32×10^{-4} to 9.4×10^{-5}, with the extreme values appearing at the beginning and the end of the fifth cycle. (The operating system unit used for Θ is $lb/in^2/scfh$.)

Figures 7 and 8 show the predictions of eq (28) for the fifteen and the three cycles of operation, respectively. Comparison of these figures with Figures 1 and 3 indicates good agreement with the data. The statistical R^2-value is now 0.93, which shows a significant improvement over that for eq (27). Figure 9 shows the corresponding time variation of the residuals of the fit. Comparing with Figure 6, it appears that the amplitude of the residuals are reduced and the residuals now fluctuate around zero. However, a systematic and roughly periodic variations in the residuals is observable in both Figures 6 and 9. These periodic deviations appear to be associated with the statistical effect of operational changes made at the time of cycle five on the fitted correlation.

Use of the correlation given by (28) leads to an estimated cake permeability of $k_c = 8.6 \times 10^{-13}$ m^2, which is comparable with the earlier value for the idealized case. The value of filter permeability, k_f, could not be estimated because the pressure drop of the system, ΔP_o, was not measured.

Incomplete cleaning

The volume of "residual" cake remaining on the filter immediately after cleaning and the baseline pressure drop caused by this residual cake, as calculated from the incomplete filter-cleaning model [eq (19)], are illustrated in Figure 10. Results are included for 1%, 5%, or 10% of the cake left on the filter after each cleaning. For $^r f = 0.01$, after 70 cleaning cycles (i.e., 35 hr, if t' = 1/2 hr) the cake volume after cleaning is about 1/2 the volume of cake deposited during one filtration cycle. For $^r f = 0.05$, after 70 cleaning cycles the cake volume after cleaning is almost 4 times the volume of cake deposited during one filtration cycle. And if $^r f = 0.10$,

the volume of cake left after cleaning is about 10 times the volume of cake deposited during one filtration cycle. To a first approximation, more-frequent cleaning will extend the time-to-shutdown only if it reduces ^{r}f (e.g., by reducing the cake sintering time and cake strength).

Re-entrainment

Counter-intuitive insights into the effects of re-entrainment on filter-cake thickness and tubesheet pressure drops can be obtained by examining the effects of different fractions of re-entrainment in the constant-fraction re-entrainment model [eq (26)]. Figure 11 illustrates the behavior of $(\Delta P - \Delta P_o)/\Delta P'$ versus *t*, as predicted for 25%, 50%, 75%, and 90% re-entrainment fractions. Although re-entrainment of 25% of the removed cake may seem substantial, its effects on the pressure drop and cake thickness are not large; this degree of re-entrainment increases the baseline pressure drop by slightly less than half of $\Delta P'$ (i.e., the maximum cake-induced pressure drop, if no re-entrainment occurs). Likewise, the additional cake thickness caused by the re-entrainment is less than 1/2 the thickness of the cake just before cleaning, if no re-entrainment occurred. For 25% re-entrainment, the approach to these asymptotic limits is very rapid, being almost complete after two cycles. As the re-entrainment fraction increases, both the asymptotic limit and the time required to approach this limit increase. For 50% re-entrainment, the maximum pressure drop (and cake thickness) are doubled by the re-entrainment. For 75% re-entrainment the maximum cake thickness is quadrupled, and for 90% re-entrainment the cake thickness and pressure drop increase nine-fold. Even for this extreme degree of re-entrainment, the approach to steady-state operation is very rapid compared to the required operating time of the filter system.

Evaluation of f's

The Θ_i term was introduced in the model equation given by (28) to account for the changes in the baseline differential pressure after each backpulse. These are equal to the differences between the initial pressure drops in consecutive cycles normalized by the volumetric gas flow rate. Thus, for the jth cycle,

$$\Theta_{j+1} = [^{i}(\Delta P_{j+1}) - {}^{i}(\Delta P_j)]/Q, \tag{29}$$

where $^{i}(\Delta P)_j$ is the baseline pressure drop in the jth cycle given by (22b). It then follows that

$$\Theta_{j+1} = [f_{j+1}\ {}^{e}(\Delta P_j) - f_j\ {}^{e}(\Delta P_{j-1})]/Q. \tag{30}$$

Here $^{e}(\Delta P)_j$ is the pressure drop at the end of the jth cycle before the backpulse. Assuming that eq (21) holds, we find

$$\Theta_j = (f_j - f_{j-1})\ (\Delta P')/Q, \tag{31}$$

from which f_j may be evaluated as

$$f_j = f_{j-1} + \Theta_j\ Q/\Delta P'. \tag{32}$$

Equation (32) provides an iterative expression for determining the values of *f*. As was noted before, the values of Θ could be positive or negative. The positive values of Θ indicate an increase in the cake thickness due to re-entrainment and/or incomplete cleaning. The negative values of Θ correspond to the cases that the backpulse causes part of the residual cake buildup from the earlier cycles together with the one of the current cycle to be removed.

CONCLUSION

The presented results indicate that the simple filter model together with appropriate statistical fits may be used to capture the main features of the MGCR filter vessel pressure drop variations. The results may also be used to estimate the filter cake permeability. Such information could provide a semi-empirical procedure for estimating the filter cake thickness during the operation of the filter vessel.

The analyses of MGCR data indicate the importance of simultaneously measuring particle concentrations as well as gas-flow rates and tubesheet pressure drops. The analyses also suggest that computer control of cleaning backpulses may be important to maintain accurate reproducibility and measurement of the length of the filtration cycle.

It might seem that re-entrainment should cause the tubesheet pressure drop and filter-cake thickness to increase without limit, but the results presented here indicate that this is not necessarily so. So long as no more than about 25% of the cake fragments are re-entrained, the pressure-drop increases caused be re-entrainment should be acceptable. The calculations indicate that for re-entrainment the approach to "stable" (i.e., asymptotic-limit) operation occurs relatively rapidly. Re-entrainment should be a problem only if more than 1/2 of the cake removed by each backpulse is re-entrained. For the incomplete filter-cleaning model presented, however, the pressure drop and cake thickness do increase without limit, and stable operation never is achieved.

The difference between stable and unstable operation is this: In unstable operation the amount of cake permanently removed by the filter-cleaning step was a constant fraction of the cake deposited *during that cycle*; in stable operation, the amount of cake permanently removed by each backpulse was a constant fraction of the *total cake present* just before cleaning. The crucial difference is, that in the latter case, as the total amount of accumulated cake increases, the amount of cake removed by cleaning also increases; hence, an asymptotic limit exists. If the absolute amount of cake removed by each cleaning stays constant (or decreases) as filter cake accumulates over multiple cycles, stable filter-system performance cannot be achieved.

NOMENCLATURE

a	=	inside filter radius
b	=	outside filter radius
c	=	proportionality constant between ΔP_o and Q^2
f	=	fraction of filter-cake fragments re-entrained (in constant re-entrainment fraction model)
^{r}f	=	fraction of filter-cake not removed by a cleaning backpulse
f_j	=	fraction of filter-cake fragments re-entrained during jth cycle

h	=	filter length
k_c	=	filter-cake permeability
k_f	=	filter permeability
n	=	number of filters
t	=	time (measured from the time of backpulse)
T_s	=	limiting operation time
B	=	outside filter-cake radius
B_{max}	=	filter-cake radius at which bridging occurs
F	=	volume fraction of particulates in incoming gas/particle stream
N	=	number of filtration cycles
ΔP	=	total pressure drop across tubesheet
$\Delta P'$	=	increase of pressure drop across cake during one cycle
ΔP_f	=	pressure drop across (clean) filter
ΔP_o	=	total pressure drop minus pressure drop across filters and filter cakes
Q	=	(volumetric) gas flow rate
R	=	resistance
μ	=	gas viscosity
ϕ	=	filter-cake porosity
ρ	=	volume-average particle density

ACKNOWLEDGEMENTS

V. Powell and E. Ibrahim were Faculty Participants under the Oak Ridge Institute for Science and Education (ORISE) program; G. Ahmadi was a Senior Associate under the National Research Council (NRC) program. This work was funded by the Office of Fossil Energy, U.S. Department of Energy.

REFERENCES

1. Mudd, M. J. and & Bauer, D. A., (1987) Proceedings 1987 International Conference on Fluidized Bed Combustion, ASME, Ed. Mustonen, J.P., pp. 256-260.

2. Clift, R. and Seville, J.P.K., (1993) Gas Cleaning at High Temperatures, Blackie Academic & Professional, New York.

3. Thambimuthu, K.V., (1993) Gas Cleaning for Advanced Coal-Based Power Generation, IEACR/53, IEA Coal Research, London.

4. Yang, W.C., Newby, R.A., Lippert, T.E. and Cicerco, D.C., (1995) "Westinghouse Advanced Particle Filter System," in Proceedings of Advanced Coal-Fired Power System '95, U.S. Department of Energy, Morgantown Energy Technology Center, Morgantown, WV, June 27-29.

5. Lippert, T.E., Bruck, G.J. Sanjana, Z.N. and Newby, R.A. (1995) "Westinghouse Advanced Particle Filter System," in Proceedings of Advanced Coal-Fired Power System '95, U.S. Department of Energy, Morgantown Energy Technology Center, Morgantown, WV, June 27-29.

FIGURES

Figure 1. Variation of operational data, $\Delta P/Q$ versus t, for the filter vessel of the MGCR (gasification) unit.

Figure 2. Variation of operational data, Q versus t, for the filter vessel of the MGCR (gasification) unit.

Figure 3. Variation of operational data, $\Delta P/Q$ versus t, for the filter vessel of the MGCR (gasification) unit.

Figure 4. Variation of $\Delta P/Q$ with time as calculated from equation (27).

Figure 5. Variation of $\Delta P/Q$ with time as calculated from equation (27).

Figure 6. Residuals from the fit of equation (27) to the operation data of Figure 1.

Figure 7. Variation of $\Delta P/Q$ with time as calculated from equation (28).

Figure 8. Variation of $\Delta P/Q$ with time as calculated from equation (28).

Figure 9. Residuals from the fit of equation (28) to the operation data of Figure 1.

Figure 10. Filter-cake thickness and pressure drop, $\Delta P - P_o$, versus t for the case of constant-fraction incomplete filter cleaning and no re-entrainment.

Figure 11. $(\Delta P - \Delta P_o)/\Delta P'$ versus t, as predicted by the constant-fraction re-entrainment model [eq (26)], for different fractions of re-entrainment.

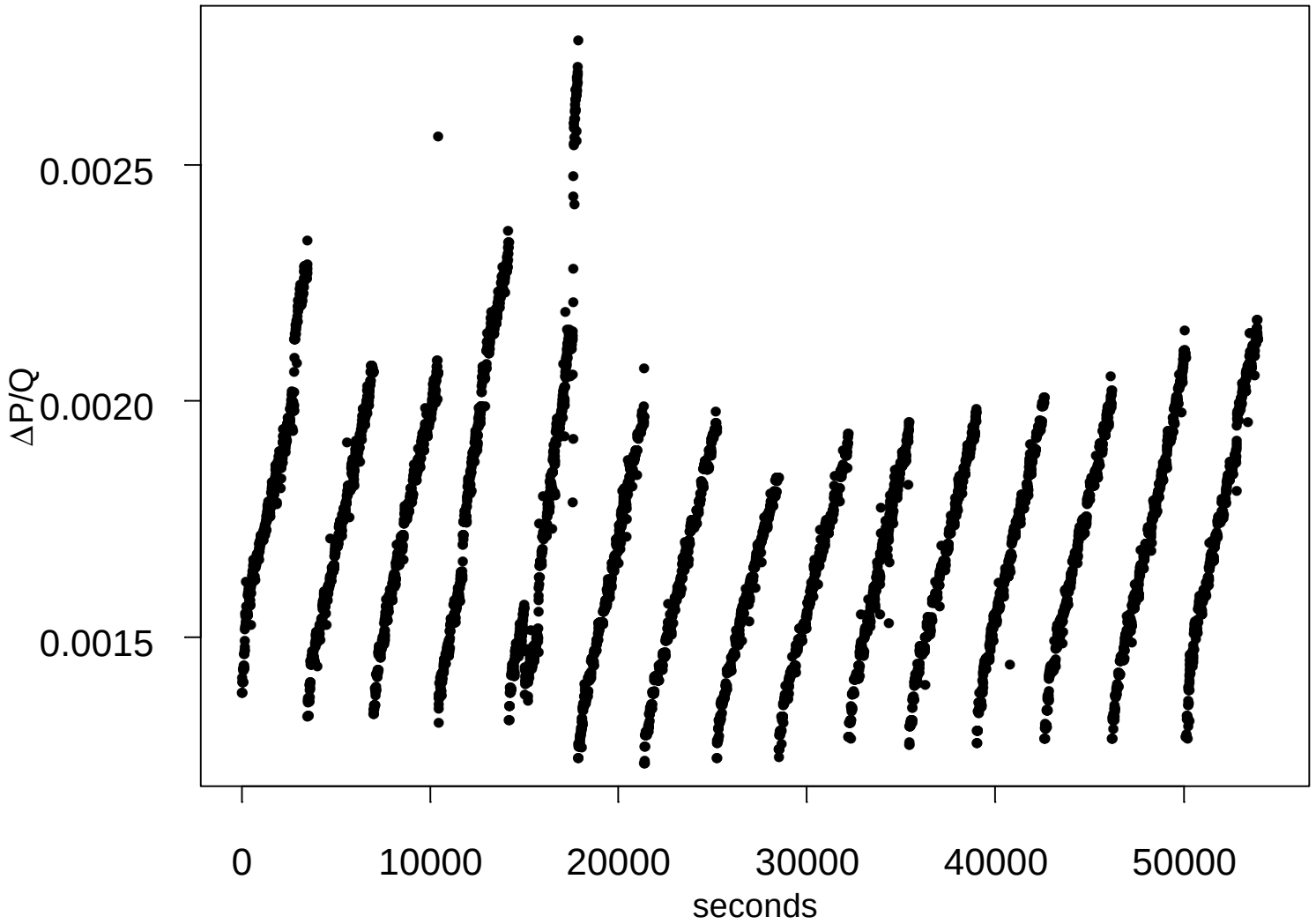

Figure 1. Variation of operational data, ΔP/Q versus t, for the filter vessel of the MGCR (gasification) unit.

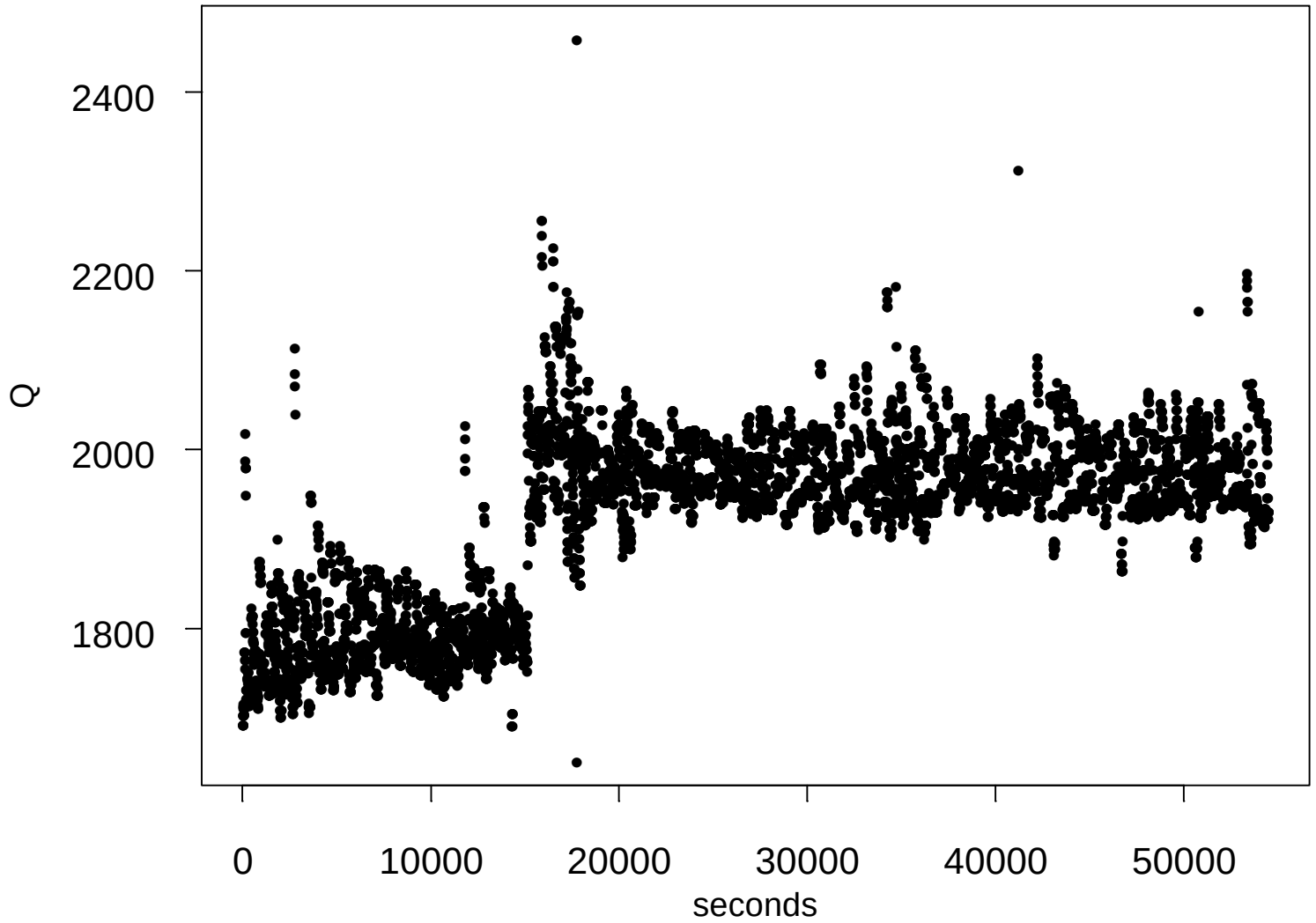

Figure 2. Variation of operational data, Q versus t, for the filter vessel of the MGCR (gasification) unit.

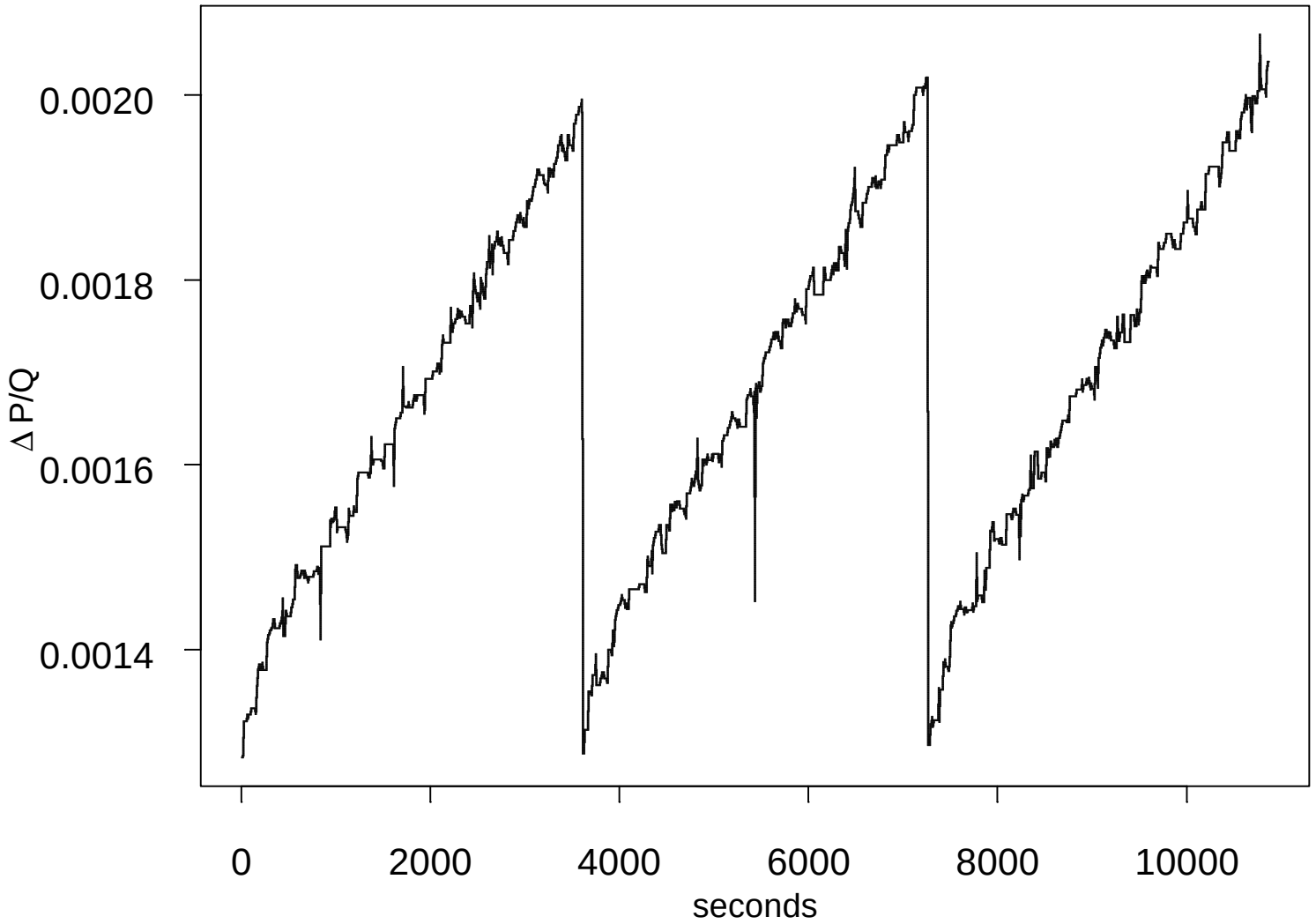

Figure 3. Variation of operational data, ΔP/Q versus t, for the filter vessel of the MGCR (gasification) unit.

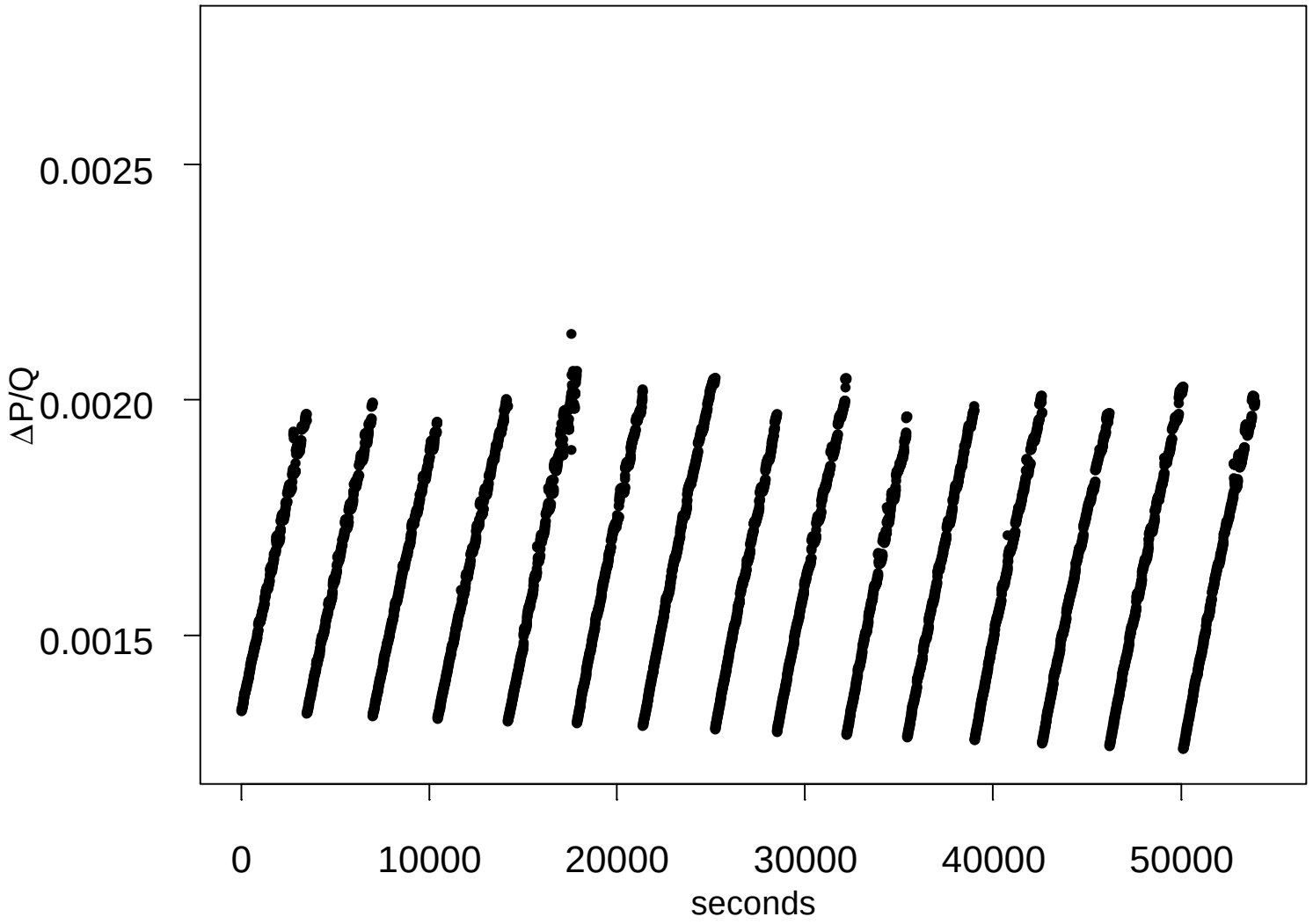

Figure 4. Variation of ΔP/Q with time as calculated from equation (27).

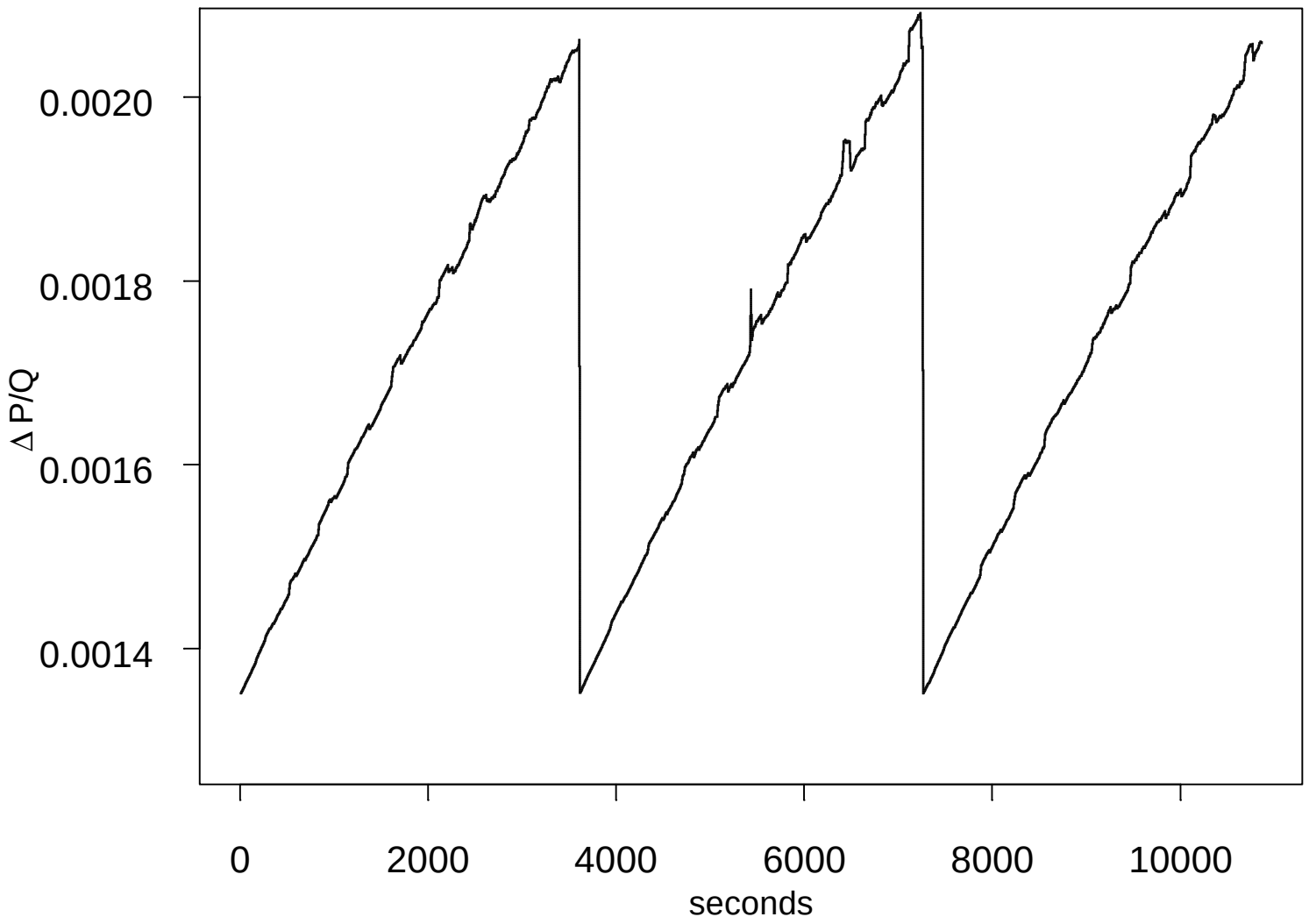

Figure 5. Variation of ΔP/Q with time as calculated from equation (27).

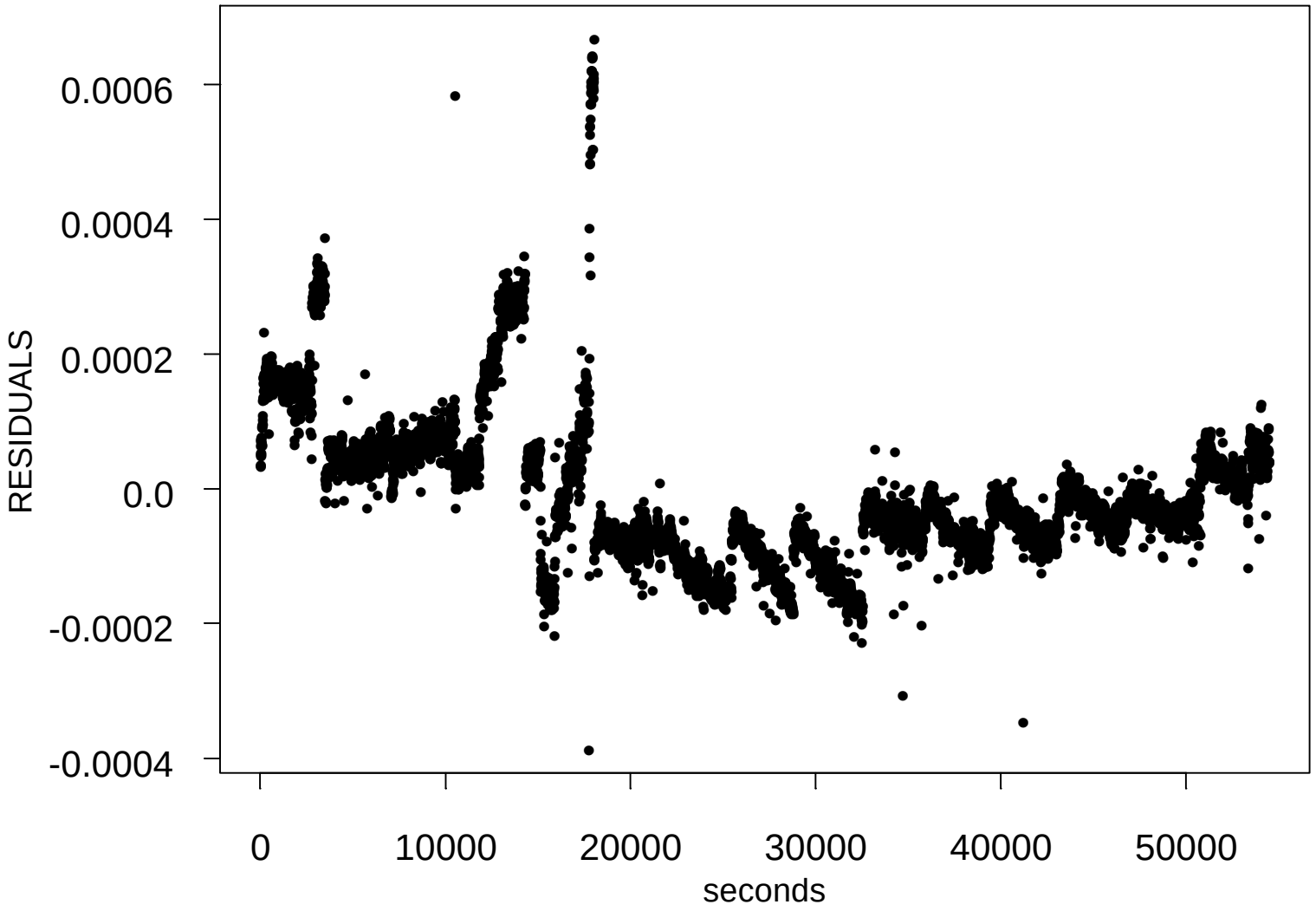

Figure 6. Residuals from the fit of equation (27) to the operation data of Figure 1.

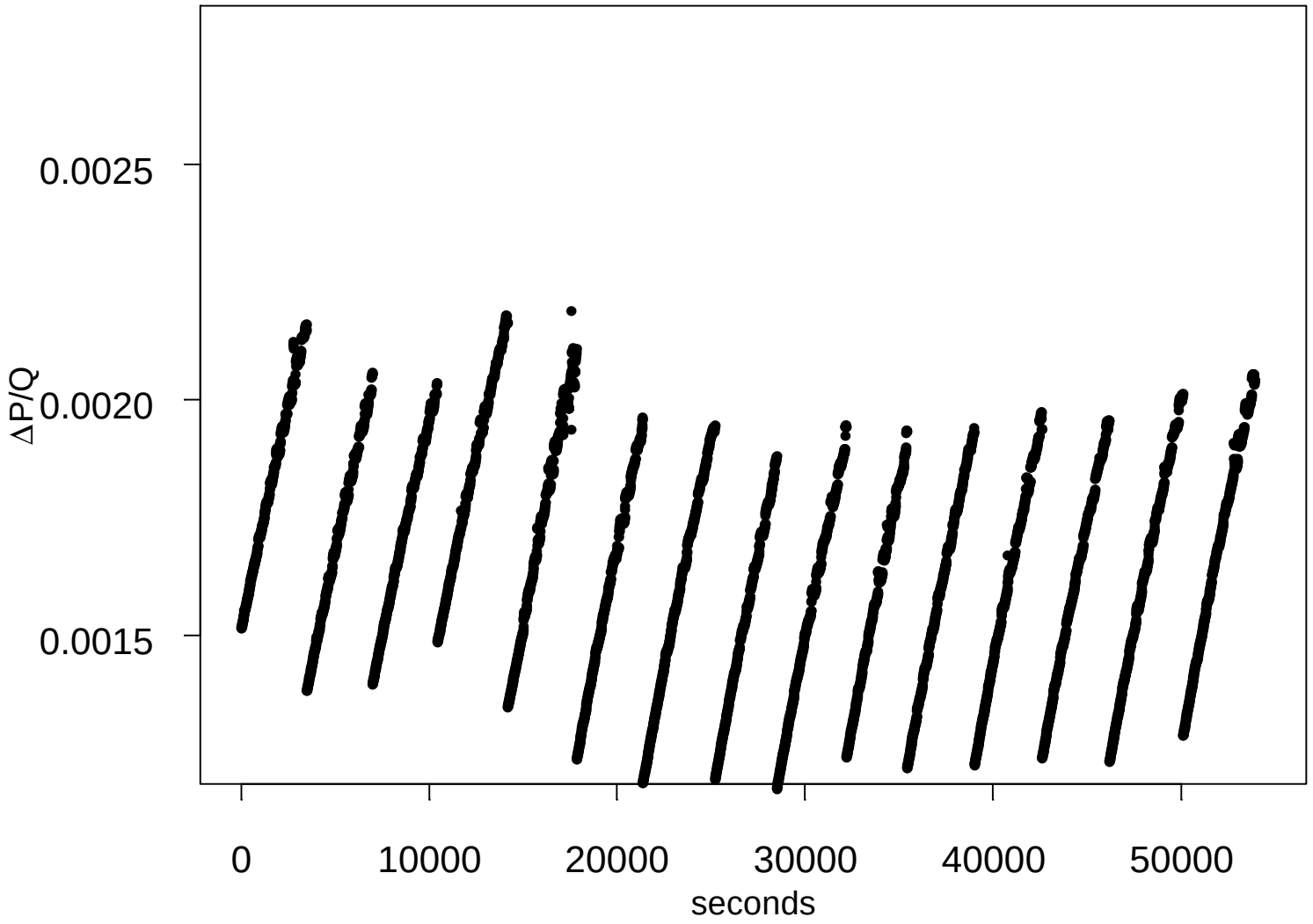

Figure 7. Variation of ΔP/Q with time as calculated from equation (28).

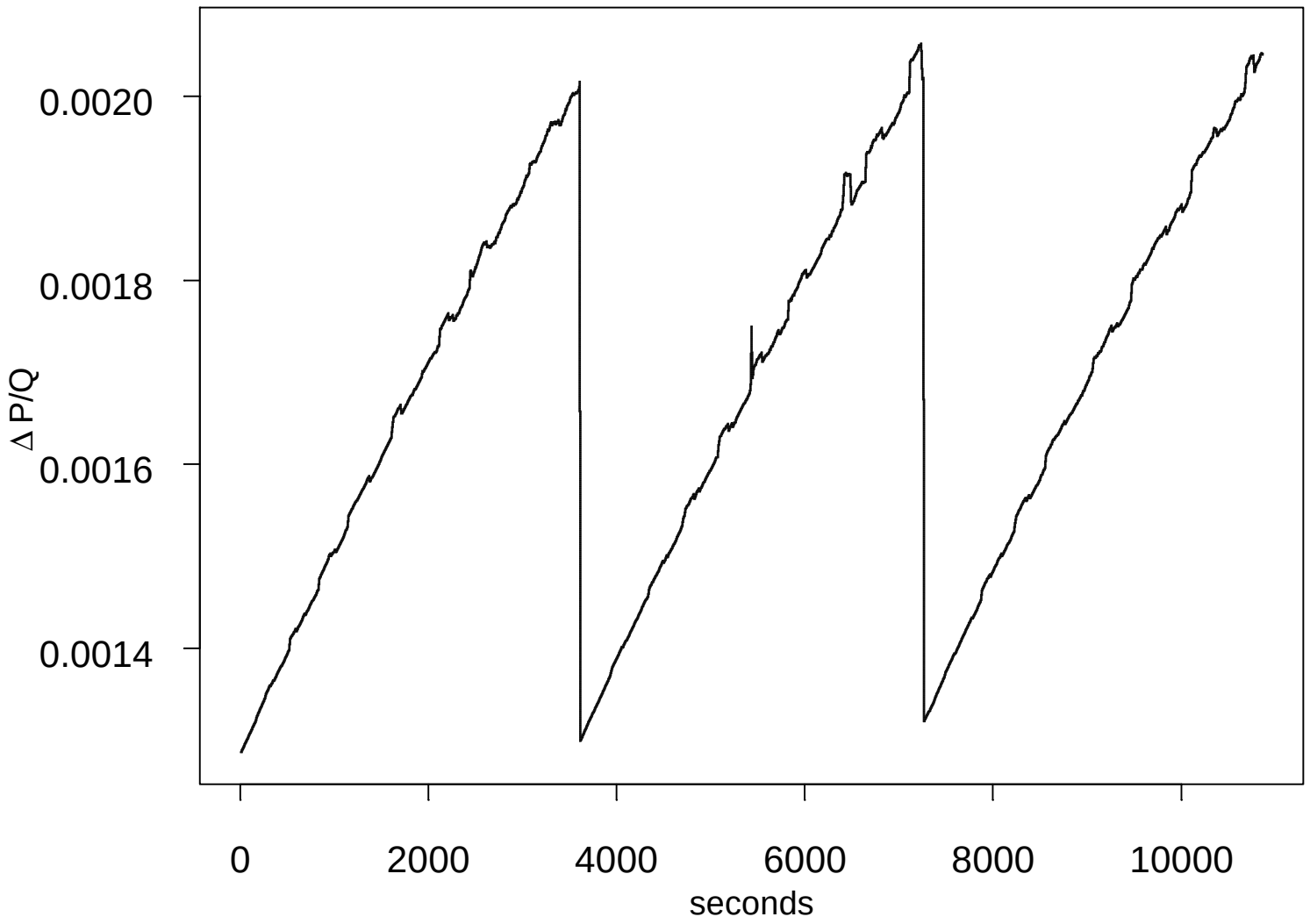

Figure 8. Variation of ΔP/Q with time as calculated from equation (28).

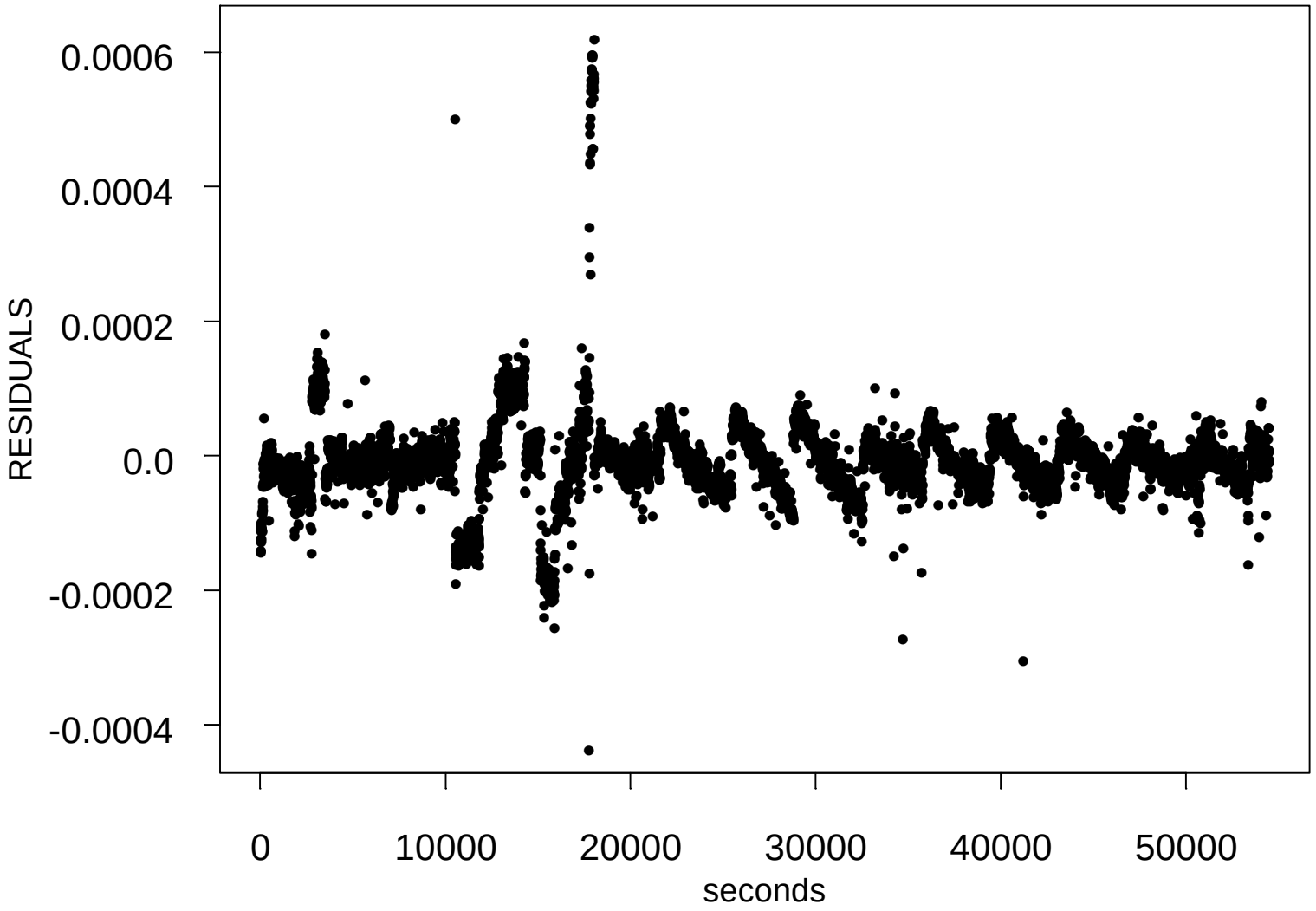

Figure 9. Residuals from the fit of equation (28) to the operation data of Figure 1.

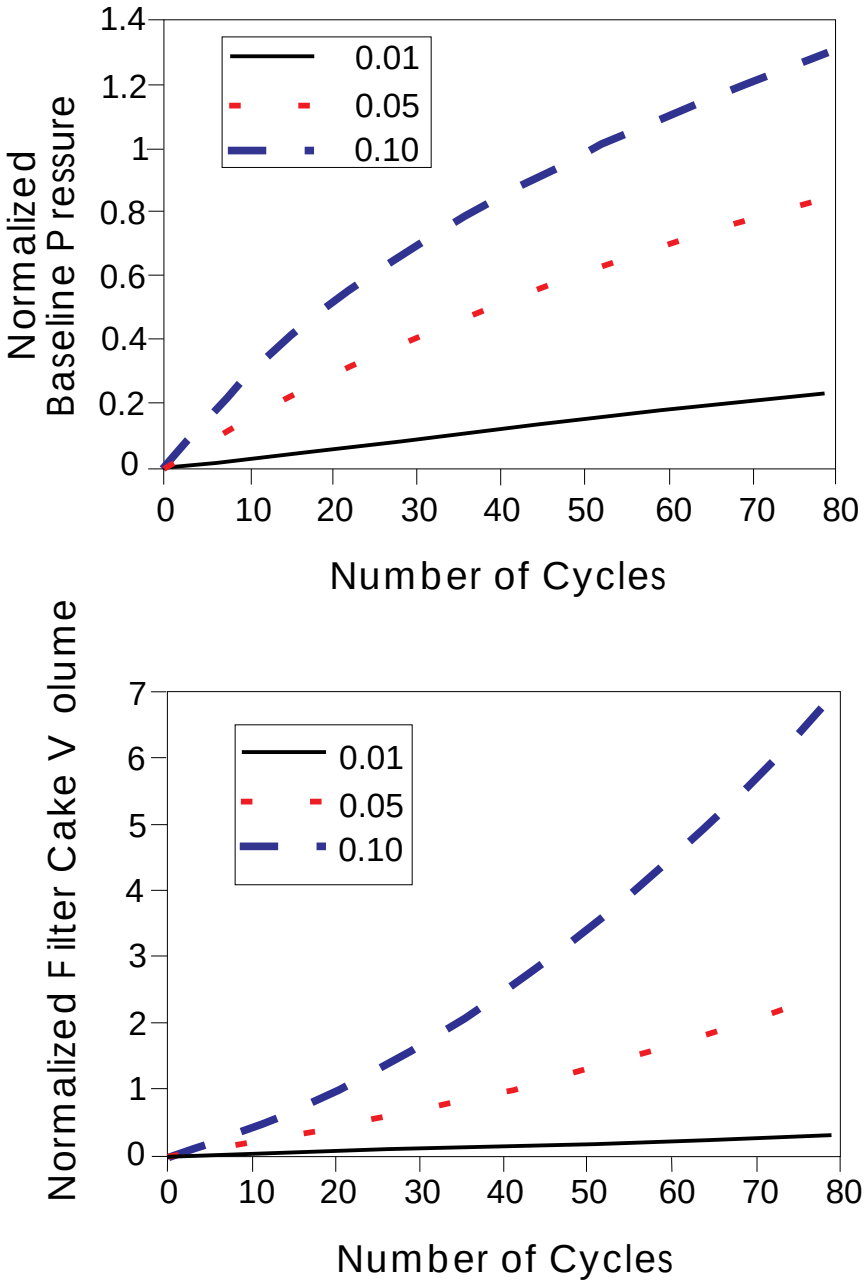

Figure 10. Filter-cake thickness and pressure drop, $\Delta P - P_0$, versus *t* for the case of constant-fraction incomplete filter cleaning and no re-entrainment.

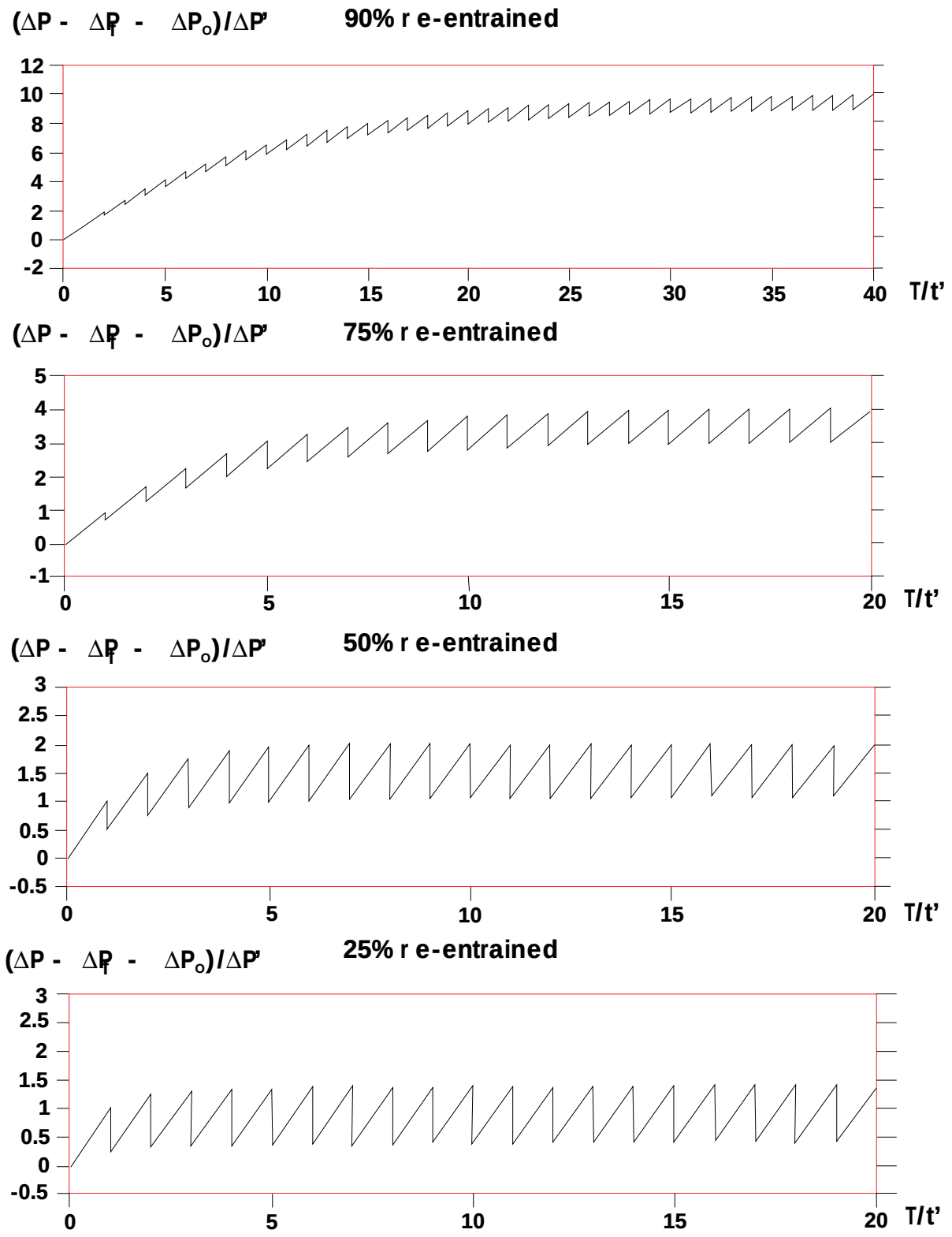

Figure 11. $(\Delta P - \Delta P_0)/\Delta P'$ versus *t*, as predicted by the constant-fraction re-entrainment model [eq (26)], for different fractions of re-entrainment.